ELSEVIER

Nuclear Physics A 637 (1998) 3–14

NUCLEAR PHYSICS A

The masses of ^{70,71}Se

M. Chartier[a,1], W. Mittig[a], N.A. Orr[b], J.-C. Angélique[b], G. Audi[c], J.-M. Casandjian[a,2], A. Cunsolo[d], C. Donzaud[e], A. Foti[d], A. Lépine-Szily[a,f], M. Lewitowicz[a], S. Lukyanov[g], M. Mac Cormick[e], D.J. Morrissey[h], A.N. Ostrowski[a,3], B.M. Sherrill[h], C. Stephan[e], T. Suomijärvi[e], L. Tassan-Got[e], D.J. Vieira[i], A.C.C. Villari[a], J.M. Wouters[i]

[a] *GANIL, Bld Henri Becquerel, BP 5027, 14076 Caen Cedex 5, France*
[b] *LPC, IN2P3-CNRS, ISMRA et Université de Caen, Bld du Maréchal Juin, 14050 Caen Cedex, France*
[c] *CSNSM, IN2P3-CNRS, Bâtiment 108, 91405 Orsay Campus, France*
[d] *Dipartimento di Fisica, Universita di Catania and INFN, Corso Italia 57, 95129 Catania, Italy*
[e] *Institut de Physique Nucléaire, IN2P3-CNRS, 91406 Orsay, France*
[f] *IFUSP-Universidade de São Paulo, C.P. 66318, 05315-970 São Paulo, Brazil*
[g] *LNR, JINR, Dubna, P.O. Box 79, 101 000 Moscow, Russian Federation*
[h] *NSCL, Michigan State University, East Lansing, MI 48824-1321, USA*
[i] *Los Alamos National Laboratory, Los Alamos, NM 87545, USA*

Received 16 April 1998; accepted 6 May 1998

Abstract

The masses of the neutron-deficient nuclei ^{70,71}Se have been measured using a direct time-of-flight technique following the fragmentation of a ^{78}Kr beam (73 MeV/nucleon). Mass excesses of -62.31 ± 0.35(syst.) ± 0.30(stat.) and -63.49 ± 0.25(syst.) ± 0.20(stat.) MeV, respectively, were deduced. In addition, a novel technique based on stripping was developed for the purification of heavy fragmentation beams. This technique provides a good selectivity – typically isotopes of a single Z are transmitted – without altering the beam quality. © 1998 Elsevier Science B.V.

PACS: 21.10.Dr; 27.50.+e

[1] Corresponding author; present address: NSCL, Michigan State University, East Lansing, MI 48824-1321, USA; e-mail: chartier@nscl.msu.edu.
[2] Present address: Nuclear Physics Laboratory, University of Washington, Seattle, WA 98195, USA.
[3] Present address: Dept. of Physics and Astronomy, The University of Edinburgh, EH9 3JZ, UK.

PII S0375-9474(98)00228-0

1. Introduction

Much interest has been recently centered on the very neutron-deficient nuclei in the mass region $A \approx 60$–80. One of the major motivations of such studies is the nuclear structure of $N \simeq Z$ nuclei near the proton drip-line in a region of shape transition [1,2]. Mass systematics may provide an important guide in understanding such effects. At a more fundamental level, mass measurements for nuclei far from stability provide a crucial test of the predictive powers of a variety of mass models which for the most part are constrained by nuclei near stability.

Interest in this region has also arisen from the possible role played by these nuclei in astrophysical events such as X- and γ-ray flashes [3]. In particular, the drip-line (and near drip-line) nuclei in this region are believed to provide the pathway at high mass for the so-called rapid proton (rp-) capture process [4] (at lower mass, $A < 40$, the pathway is adjacent to the line of stability). This process is believed to take place[4] in environments such as the accretion of material onto a neutron star from a companion in a binary system during explosive hydrogen burning [7]. Recent studies [8–12] have begun to map the drip-line in this mass region and thus provide constraints on the possible pathways and termination point of the rp-process. In particular, the recent evidence of the instability against particle emission of ^{69}Br [12] implies that the rp-process is significantly slowed down at ^{68}Se, the half-life of which is comparable to the expected time scale of the process.

Scant experimental information is available on the masses of nuclei in this region [13], particularly at the drip-line itself. This is mainly due to the difficulty in producing these nuclei – for nuclei below $A \approx 60$ the masses are better known due to the proximity of the drip-line to the line of stability. Presently, the results of global calculations and systematics of the nuclear mass surface are used to estimate the various reaction rates involved in modeling the rp-process (proton capture, photodisintegration and β-decay). Measuring the masses of key nuclei at the drip-line or close to it is thus important for an accurate modeling of the rp-process [7].

2. Experimental techniques

2.1. Mass measurement

The direct time-of-flight, magnetic rigidity mass measurement technique employed here has been used in a series of experiments [14–16] which to date have concentrated on light ($A < 40$) neutron-rich nuclei. This method exploits the long flight-path ($\sim$ 100 m) available at GANIL between the α-spectrometer and the SPEG spectrograph [17]. The method consists of measuring the magnetic rigidity $B\rho$ and the time-

[4] It should be noted that very recent observation of the optical counterparts of γ-ray bursts indicate that such events occur at cosmological distances rather than within our galaxy [5,6]. Such events would then require processes much more violent than explosive hydrogen burning.

of-flight 'ToF' of ions of charge state q traversing a known flight-path L of an achromatic system. The mass m of the ions can be deduced from the expression

$$B\rho = \frac{mv}{q} = \frac{m}{q} \cdot \frac{L}{\mathrm{ToF}}. \tag{1}$$

The achromatic system comprised the beam line from the exit of the α-spectrometer to the focal plane of SPEG. Using this method, the measurement of the mass m of an ion ${}^{A}_{Z}X^{q+}$ thus requires the measurement of the time-of-flight and the magnetic rigidity. The resolving power that can be achieved depends on the time-of-flight and magnetic rigidity measurement resolutions. The mass resolution obtained in previous experiments with neutron-rich nuclei was of the order of 10^{-4}.

It has been demonstrated by earlier experiments [8,11,12] that a relatively high-energy, high-intensity ^{78}Kr beam and a mass separator can be used to reach nuclei close to the proton drip-line. In the present experiment, a $^{78}Kr^{34+}$ (1 eμA) beam at 73 MeV/nucleon bombarded a 90 mg/cm^2 thick ^{nat}Ni target located between the two superconducting solenoids of the SISSI device (Source d'Ions Secondaires à Solénoïdes Supraconducteurs Intense) [18]. The choice of a nickel target was based on earlier results which demonstrated that nucleon transfer is still important at these energies – isotopes of both Rb and Sr were, for example, produced from a ^{78}Kr beam [8]. The reaction products were subsequently selected (see below) using the alpha-shaped beam analysis device (α-spectrometer) and transported to the focal plane of the SPEG spectrometer.

The time-of-flight (ToF $\sim$ 1 μs) was measured between a fast microchannel-plate detector located at the exit of the α-spectrometer and a silicon detector at the focal plane of SPEG. The measurement of the magnetic rigidity was performed via a position measurement in the bend plane of the SPEG spectrometer, using a position-sensitive microchannel-plate detector (μch) [19] located at the intermediate dispersive image plane of the analysing magnet, before the two dipoles. Drift chambers (DC) located at the focal plane were used to determine the trajectories of the ions and hence provide for the correction of second order aberrations in the system. The time and spatial resolutions were determined as 250 ps (microchannel-plate detector) and 150 ps (silicon detector), and 1 mm (μch) and 0.2 mm (DC), respectively. Particle identification was obtained in the focal plane of SPEG, in addition to the time-of-flight measurement, from a cooled silicon detector telescope that consisted of three detectors measuring the energy loss of the ions (ΔE_1 50 μm, ΔE_2 150 μm, ΔE_{xy} 163 μm) and one detector measuring the residual energy (E 4.5 mm). Two high-efficiency germanium detectors located on each side of the silicon detector telescope also permitted a check on the population of isomeric states as well as confirmed the particle identification via the observation of known isomers.

2.2. Purification by stripping

More than 200 different nuclides are produced in the fragmentation reaction ^{78}Kr (30 pnA, 73 MeV/nucleon) + ^{nat}Ni, with a total rate of $\sim 6 \times 10^5$ ions/s according to estimates given by the codes INTENSITY [20] and LISE [21]. Silicon detectors cannot withstand such high counting rates, however the maximum beam intensity was required to produce the most exotic nuclei. Thus it was necessary to purify the secondary beams to reach reasonable counting rates for the nuclei of interest. In previous experiments with neutron-rich nuclei counting rates were low enough and no other selection than by magnetic rigidity was necessary. A large number of reference masses were then available together with the unknown masses to be determined.

At intermediate energies purification is performed using a thick achromatic degrader [22]. Such a method, however, increases the beam emittance due to the energy and angular straggling in the degrader. Therefore, another purification method of the secondary ion beams was used, based on the stripping of the ions, which does not alter the optical quality of the beam.

A thin layer ($\sim$ 100 μg/cm^2) of tantalum was evaporated on the downstream face of the nickel target in order to increase the yield of ions produced in the $q = Z - 1$ charge state. Typically, at energies of 60–70 MeV/nucleon about 50% of the ions of $Z \sim 25$–35 are produced in the $q = Z - 1$ charge state with tantalum. Additionally, a thin mylar stripping foil ($\sim$ 1 mg/cm^2) was mounted between the two dipole stages of the α-spectrometer at the intermediate dispersive focal plane in order to strip off the remaining electron. Setting asymmetrically the two sections of the α-spectrometer not only eliminated the more prolific lighter nuclei, but also provided a strong selectivity based on the atomic number.

Writing the settings of the first and second parts of the α-spectrometer as

$$B\rho_1 = \frac{mv}{q_1}, \tag{2}$$

and

$$B\rho_2 = \frac{mv}{q_2}, \tag{3}$$

with

$$q_1 = Z - 1$$

and

$$q_2 = q_1 + 1 = Z,$$

the change in magnetic rigidity selects one charge state, which is equivalent (since the nuclei are fully stripped after the foil) to the selection of *one* Z value as shown in the following relation:

$$\frac{\Delta B\rho}{B\rho} = \frac{1/q_1 - 1/q_2}{1/q_1} = \frac{1}{Z}. \tag{4}$$

The resolution of two neighbouring charges,

$$\Delta\left(\frac{\Delta B\rho}{B\rho}-\frac{\Delta B\rho'}{B\rho'}\right)=\frac{1}{Z}-\frac{1}{Z+1}\sim\frac{1}{Z^2}\,, \tag{5}$$

is of the order of 0.1% for $Z \sim 30$ which corresponds to the resolution of the α-spectrometer when combined with SISSI.

A relatively large number of well-established reference masses are needed in the vicinity of the nuclei of interest for calibration and determination of the unknown masses by interpolation and/or extrapolation. Thus, the region between $Z = 30$ and $Z = 36$ was covered in the present experiment. The selection of another Z value is obtained by changing only the magnetic rigidity $B\rho_1$ of the first half of the α-spectrometer *without* retuning the beam line between the stripper and SPEG. Given the very high precision required in the measurements ($\sim 10^{-6}$), it is imperative that the experimental conditions, in particular that of the beam transport ($B\rho_2$), do not change throughout the experiment.

Calculations using the codes INTENSITY and LISE predicted a total rate of $\sim 5 \times 10^3$ ions/s with this purification method – a reduction of two orders of magnitude compared to the rate expected without any purification. Fig. 1 shows the results of calculations with INTENSITY for the fragmentation reaction ^{78}Kr + ^{nat}Ni, (a) without stripping the fragments in the α-spectrometer, and (b) after setting the α-spectrometer in order to strip ^{66}As from $q_1 = 32+$ to $q_2 = 33+$. The efficiency of this method depends on the probability of producing the ions in the initial charge state $q_1 = Z - 1$ times the q_1 to $q_2 = Z$ stripping probability (it is impossible to apply this method to light nuclei since they are produced fully stripped at these energies). A factor of 2 to 3 is lost in transmission for nuclei above $Z \sim 25$ with this method, whereas for lighter nuclei the standard thick-degrader method is more appropriate.

The method is illustrated in Fig. 2 for a secondary beam composed of different charge states observed in the SPEG dispersive focal plane during a test experiment. The different charge states produced after the passage through a thin foil are separated in the focal plane and can be selected using slits.

Fig. 3 shows examples of identification spectra obtained for different Z selections in the present experiment, including that accumulated over several different settings of the first half of the α-spectrometer. The panels (a) and (b) demonstrate that one Z line may be selected. Some nuclei with $q_2 = Z + 1$ and $q_2 = Z - 1$ are observed, indicating that the resolution was somewhat poorer than expected (possibly due to instabilities in the primary beam).

3. Mass determinations for ^{70}Se and ^{71}Se

The absolute time-of-flight (T_{abs}) was determined from both timing signals of the detectors *start* (T_{start}) and *stop* (T_{stop}) measured with respect to a common reference signal delivered by a timing calibrator (*TC*) that was not correlated with the beam

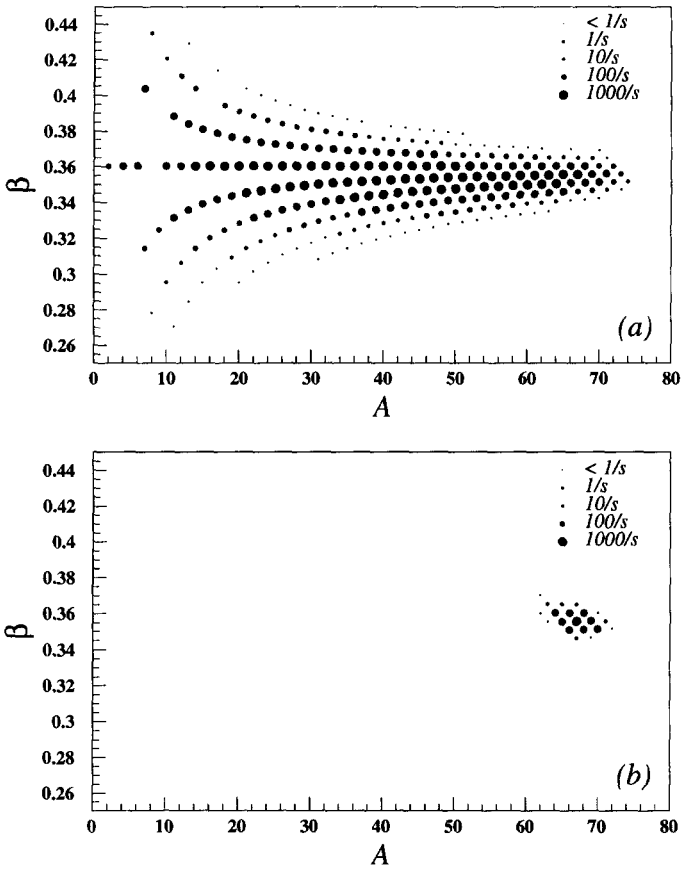

Fig. 1. INTENSITY calculations for the fragmentation reaction ^{78}Kr (30 pnA, 73 MeV/nucleon) + ^{nat}Ni. Two-dimensional plot of the reduced velocity $\beta = v/c$ as a function of the mass number for two cases: (a) predictions for the counting rate of fragments without stripping in the α-spectrometer. The total rate is estimated to $\sim 6 \times 10^5$ ions/s; (b) predictions when the α-spectrometer is set for stripping ^{66}As from $q = 32+$ to $q = 33+$. The total rate is then reduced to $\sim 5 \times 10^3$ ions/s.

(i.e., random with respect to the beam time structure). The expression for the absolute time-of-flight is given by

$$T_{\text{abs}} = T_{\text{start}} - T_{\text{stop}} + N_{TC} \cdot TC + \Delta T_o \,, \tag{6}$$

where ΔT_o is a constant and $TC = 80$ ns is the generator period. For the different ions the absolute time-of-flight is actually distributed over several periods identified with N_{TC}.

The two position measurements, $x_{\mu ch}$ and x_{DC}, determined the momentum deviation δ from the central momentum, such that the magnetic rigidity is given by

$$B\rho = B\rho_o \cdot (1 + \delta) \,, \tag{7}$$

where $B\rho_o$ is the magnetic rigidity of the central trajectory.

In the analysis, this momentum deviation was applied to the absolute time-of-flight to give a corrected time-of-flight of

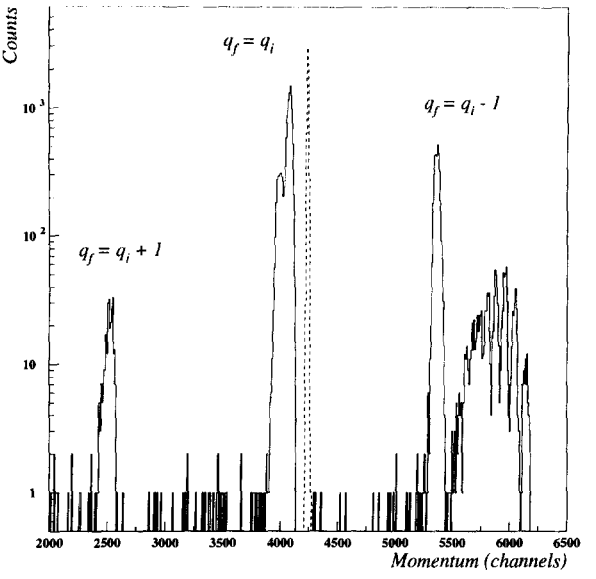

Fig. 2. A secondary beam containing different charge states, as observed in the focal plane of SPEG. The dashed line shows the momentum distribution of the beam without any foil, the full line shows the same beam when a thin foil ($\sim$ 1 mg/cm^2) is located in the beam line before the spectrometer to induce charge state changes.

$$T_{\mathrm{corr}} = T_{\mathrm{abs}} \cdot (1 + \delta)\,, \tag{8}$$

where δ is adjusted in order to minimize the corrected time-of-flight so that T_{corr} is not correlated with the position measurements,

$$\frac{\partial T_{\mathrm{corr}}}{\partial x_{\mu ch}} = \frac{\partial T_{\mathrm{corr}}}{\partial x_{DC}} = 0\,. \tag{9}$$

Standard particle-identification functions were used to select fully stripped ions ($q_2 = Z$). The mass is

$$m_o = \sqrt{1 - \beta^2} \cdot Z \cdot T_{\mathrm{corr}}\,, \tag{10}$$

with

$$\beta = \frac{v}{c} = \frac{L}{c} \cdot \frac{1}{T_{\mathrm{corr}}}\,. \tag{11}$$

Fig. 4 shows the identification spectrum obtained for nuclei with $Z = 30$ to 35, and the mass spectrum for selenium nuclei ($Z = 34$). After determination of the centroids of the peaks, a conversion factor was calculated using ions of known mass ($^{66}Ga^{31+}$) as a reference. The same conversion factor was applied to all ions to obtain their experimental mass $m_{\mathrm{exp}}c^2$ in MeV.

Finally, in order to determine a calibration function all the known mass excesses $\Delta M_{\mathrm{table}}$ from the Audi and Wapstra mass table [13] were taken into account,

$$m_{\mathrm{table}}c^2 = A \times \mathrm{amu} + \Delta M_{\mathrm{table}} - Z \times m_e c^2\,, \tag{12}$$

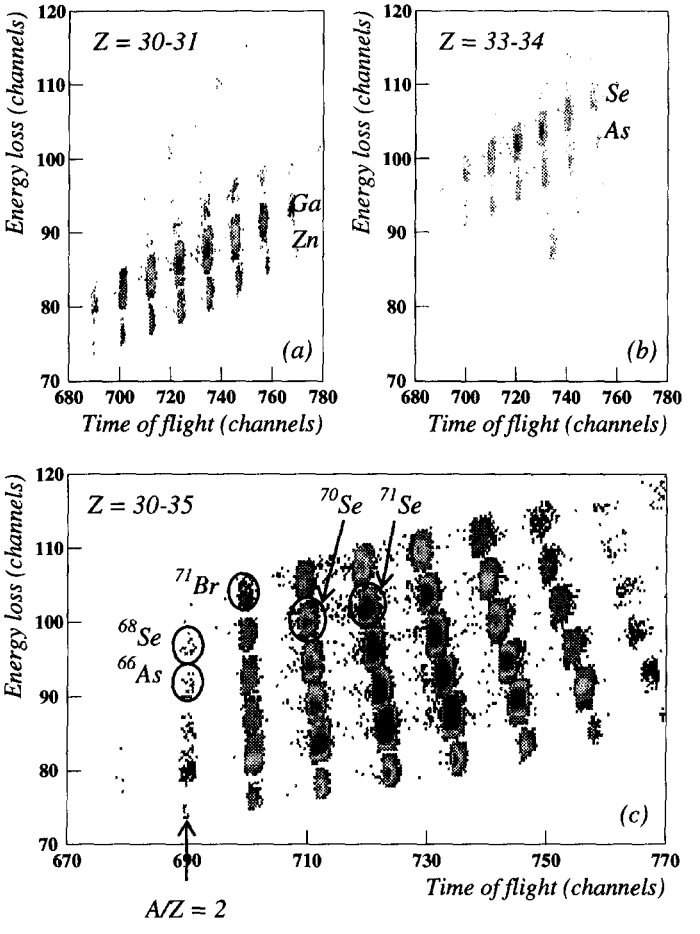

Fig. 3. Examples of identification spectra obtained for different Z selections. The upper panels (a) and (b) are optimized for one Z value ($Z = 31$ and $Z = 34$, respectively). The small number of nuclei lying one charge above $Z = 31$ on panel (a) were those selected in the charge state $q_1 = (Z + 1) - 2$. The lower panel (c) is an accumulation of data corresponding to five different settings of the first half of the α-spectrometer. It covers the area of interest including the reference masses. Nuclei without mass determinations [13] are indicated by circles.

with 1 amu = 931.494 MeV. The difference $\Delta mc^2_{\text{tab-exp}} = m_{\text{table}}c^2 - m_{\text{exp}}c^2$ between the tabulated mass and experimental mass was calculated for each detected ion. For each Z value, the points were found to lie on a straight line. Nevertheless, due to the narrow selection of ions in the α-spectrometer, each Z value actually corresponds to a different setting. Therefore, a slightly different calibration had to be used for each Z. Figs. 5 and 6 display the difference between the tabulated and experimental mass as a function of A/Z for each Z between 30 (zinc) and 35 (bromine). Nuclei without mass determinations, as indicated by the Audi and Wapstra mass table, are represented by full symbols. Most $A/Z = 2$ nuclei are not displayed owing to the very low statistics obtained in the present experiment.

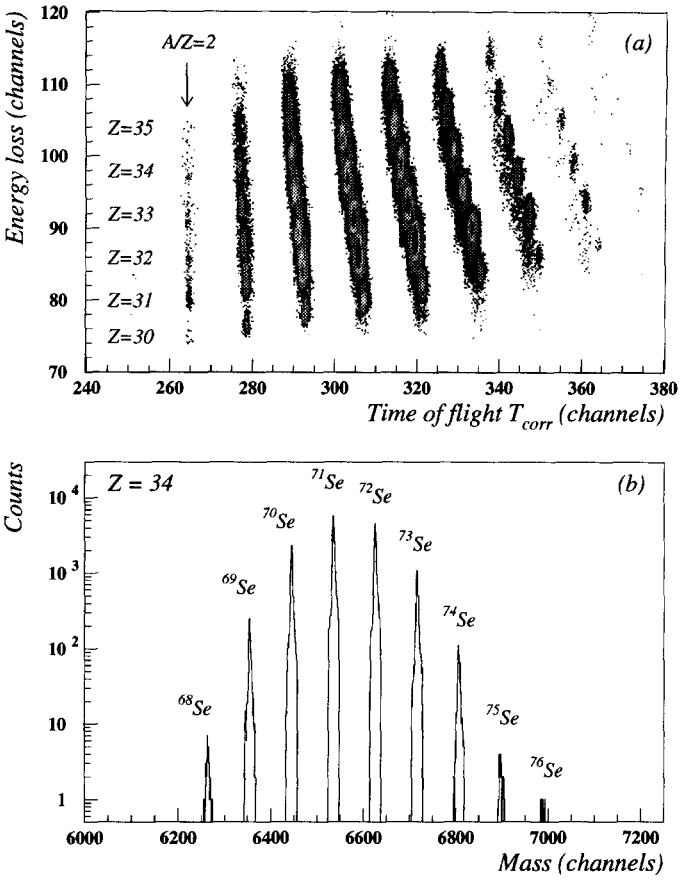

Fig. 4. (a) Identification spectrum obtained for nuclei of Z = 30–35. The time-of-flight has been corrected as discussed in the text. (b) Mass spectrum for Z = 34.

Due to the different calibration functions specifically applied for each Z value, it is not possible to use all the known masses simultaneously as reference masses, as is usually done. For each Z, corresponding to a given setting, we only have a small number of reference masses, which makes an extrapolation (such as would be necessary for ^{71}Br) to determine an unknown mass difficult. Therefore, we do not report the mass of ^{71}Br here. However, it was possible to interpolate between several known masses with reasonable precision.

In such a manner the masses of ^{70}Se and ^{71}Se, indicated by arrows in Fig. 6, have been extracted by interpolating between the known masses of ^{69}Se and of ^{72,73}Se. Assuming that no long-lived ($\tau \geq 1$ μs) isomeric states were populated, the following mass-excesses were obtained:

$$\Delta M(^{70}\mathrm{Se}) = -62.31 \pm 0.35(\mathrm{syst.}) \pm 0.30(\mathrm{stat.})\ \mathrm{MeV},$$
$$\Delta M(^{71}\mathrm{Se}) = -63.49 \pm 0.25(\mathrm{syst.}) \pm 0.20(\mathrm{stat.})\ \mathrm{MeV}.$$

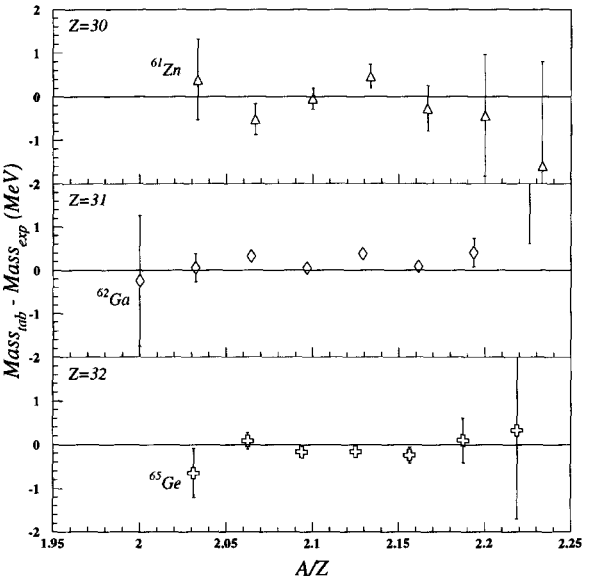

Fig. 5. Difference between the tabulated mass [13] and the experimental mass for nuclei of Z = 30–32. Error bars represent the experimental statistical errors.

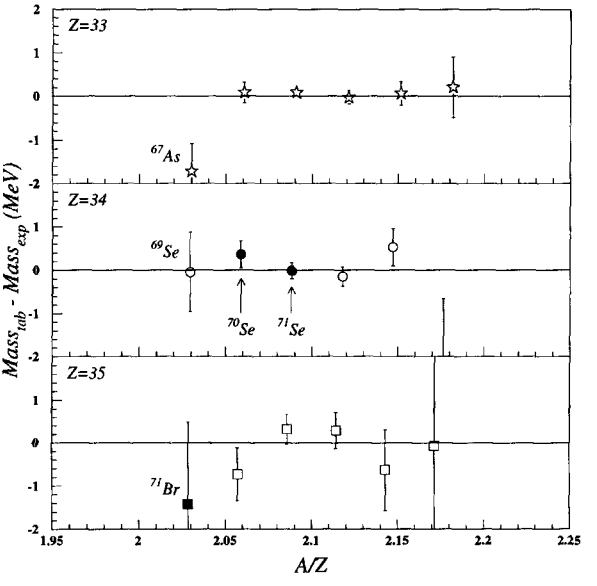

Fig. 6. Difference between the tabulated mass [13] and the experimental mass for nuclei of Z = 33–35. Nuclei without mass determinations are represented by full symbols. In these cases the systematic predictions of Audi and Wapstra are used as the tabulated mass. The isotopes ^{70}Se and ^{71}Se, whose masses have been determined in this experiment, are indicated by arrows.

Systematic errors were estimated by considering the known masses in Figs. 5 and 6. Our experimental values for ^{70}Se and ^{71}Se are very close to the interpolations of Audi and Wapstra based on systematical trends, $\Delta M(^{70}\mathrm{Se}) = -61.94 \pm 0.21$ MeV and $\Delta M(^{71}\mathrm{Se}) = -63.09 \pm 0.20$ MeV, which seem to be quite reliable in this region.

4. Conclusions

The mass excesses of ^{70}Se and ^{71}Se have been determined with precisions of 6.5×10^{-6} and 4.5×10^{-6}, respectively. These results agree well with the estimates of Audi and Wapstra based on systematical trends.

A new method for the purification of secondary beams produced by projectile fragmentation was successfully developed. This method is based on the stripping of the ions in a thin foil located between two dipole stages. It allows the selection in terms of atomic number Z, when the ions are fully stripped at the exit of the thin foil, and importantly does not increase beam emittance.

The results of this experiment indicate that the limits of the direct time-of-flight mass measurement method using the spectrometer SPEG have been reached for heavy ($A \approx 70$) nuclei, considering the required precision of a few 10^{-6}. Given the relatively high production cross sections via fusion-evaporation for neutron-deficient nuclei of $A \approx 60$–80, an alternative to the present experiment would be to use the CSS2 cyclotron technique [23–25]. Such a technique does, in principle (suitable beam-target combinations deliverable by the first GANIL cyclotron must be available), provide for much higher precision.

References

[1] C.J. Lister et al., Phys. Rev. C 42 (1990) 1191.
[2] C. Chandler et al., Phys. Rev. C 56 (1997) 2924R.
[3] R.E. Tamm, Ann. Rev. Nucl. Part. Sci. 35 (1985) 1.
[4] R.K. Wallace and S.E. Woosley, Ap. J. Suppl. 45 (1981) 389.
[5] K. Sahu et al., Nat. 387 (1997) 476.
[6] T. Galama et al., Nat. 387 (1997) 479.
[7] A.E. Champagne and M. Wiescher, Ann. Rev. Nucl. Part. Sci. 42 (1992) 39.
[8] M.F. Mohar et al., Phys. Rev. Lett. 66 (1991) 1571.
[9] S.J. Yennello et al., Phys. Rev. C 46 (1992) 2620.
[10] J.C. Batcheler et al., Phys. Rev. C 47 (1993) 2038.
[11] J.A. Winger et al., Phys. Lett. B 299 (1993) 214.
[12] B. Blank et al., Phys. Rev. Lett. 74 (1995) 4611.
[13] G. Audi and A.H. Wapstra, Nucl. Phys. A 595 (1995) 409.
[14] A. Gillibert et al., Phys. Lett. B 176 (1986) 317.
[15] A. Gillibert et al., Phys. Lett. B 192 (1987) 39.
[16] N.A. Orr et al., Phys. Lett. B 258 (1991) 29.
[17] L. Bianchi et al., NIM A 276 (1989) 509.
[18] A. Joubert, IEEE I (1991).
[19] O.H. Odland et al., NIM A 378 (1996) 149.
[20] J.A. Winger, B.M. Sherrill and D.J. Morrissey, NIM B 70 (1992) 380.

[21] D. Bazin and O. Sorlin, Programme LISE (1993), unpublished.
[22] J.-P. Dufour et al., NIM A 248 (1986) 267.
[23] G. Auger et al., NIM A 350 (1994) 235.
[24] M. Chartier et al., Phys. Rev. Lett. 77 (1996) 2400.
[25] M. Chartier et al., Proc. Conf. EMIS13 on Electromagnetic Isotope Separators and Techniques Related to their Applications, Bad Dürkheim, Germany, 1996, NIM B 126 (1997) 334.